Experimental And Theoretical Studies of Green Synthesized Cu_2O Nanoparticles Using *Datura Metel L*

Karuppaiah Chinnaiah
Kalasalingam University: Kalasalingam Academy of Research and Education
Vivek Maik
SRM-RI: SRM Research Institute Kattankulathur
Karthik Kannan
Kumoh National University of Technology: Kumoh National Institute of Technology
V. Potemkin
South Ural State University (National Research University): Uzno-Ural'skij gosudarstvennyj universitet
M. Grishina
South Ural State University (National Research University): Uzno-Ural'skij gosudarstvennyj universitet
M. Gohulkumar
Vivekanandha College of Arts and Sciences for Women
Ratnesh Tiwari
Dr CV Raman University
K. Gurushankar (gurushankar01051987@gmail.com)
Kalasalingam University: Kalasalingam Academy of Research and Education https://orcid.org/0000-0003-1173-2859

Research Article

Keywords: Datura metel L, Cu2O nanoparticles, UV, XRD, FT-IR, DFT

Posted Date: September 20th, 2021

DOI: https://doi.org/10.21203/rs.3.rs-804953/v1

Version of Record: A version of this preprint was published at Journal of Fluorescence on January 8th, 2022. See the published version at https://doi.org/10.1007/s10895-021-02880-4.

Abstract

In biomedical applications, Cu_2O nanoparticles are of great interest. The bioengineered route is eco-friendly for the synthesis of nanoparticles. Therefore, in the present study, there is an attempt to synthesis of Cu_2O nanoparticles using *Datura metel L*. The synthesized nanoparticles were characterized by UV-Vis, XRD, and FT-IR. UV-Vis results suggest the presence of hyoscyamine, atropine in *Datura metel L*, and also, nanoparticles formation has been confirmed by the presence of absorption peak at 790 nm. The average crystallite size (19.56 nm) obtained by XRD. Further, the various functional groups have been confirmed through FT-IR. To highlight the peak of the dominant frequencies, Fourier Power Spectrum was also used to analyze the synthesized nanomaterials spectrum results. Density functional theory (DFT) further also used over a period of time to measure the energy of the substance, which seems to suggest a stable compound. Furthermore, the calculated energies, thermodynamic characteristics (such as enthalpies, entropies, Gibbs-free energies), modeled structures of complexes, crystals, and clusters, and predicted yields, rates, and regio- and stereospecificity of reactions were in good agreement with the experimental ones. Overall, the findings indicate the successful synthesis of Cu_2O nanoparticles using *Datura metel L*. correlates with theoretical study.

Introduction

Now a day's engineered nanoparticles and their technological impacts are creating new revolutionary thoughts in the industrial process through the utilization of optical, electronic, and magnetic properties [1]. Cu_2O is an important promising candidate among the transition-metal oxides due to high abounded, nontoxic and cheap availability. Generally, it consists of + 1, +2 oxidation states known as cuprous and cupric ions [2]. The nanoparticles of Cu_2O is naturally P-type semiconductor material with a narrow bandgap of 1.2 and 2 eV, which could be favor on light absorption in several biomedical applications such as MRI-ultra sound dual imaging, microbial activity [3, 4] and bandgap of 2.98 eV used as a photoelectrode for solar energy conversion [5]. The synthesis of copper oxide nanoparticles via the green route is an easy production strategy and eco-friendly method [2]. Hence, green synthesis is the best adopted route for nanoparticles production when compared with the chemical method due to without requirement of any reducing and stabilizing agent. The plant metabolism like flavanoid, alkaloids, terpenoids, polyphenols, and proteins are a reservoir of plant tissue, it could be used as a reducing agent on various nanoparticles synthesis [6]. *Datura metel L.* is a Solanacae family agriculture plant that is geographically spread over on gibbous world either as an origin or foreign plant in Asia, America, and Europe. The species of *Datura metel L.* have been used as classical Chinese medicine for the treatment of asthma, coughs and antitumor activities, etc. Particularly, the major constituent of this plant namely withanolides having plant steroids build on by ergostane skeleton in the side chain of δ- lactone and their predominant alkaloid content of hyoscyamine, atropine has given the medicinal properties on nanoparticles formulation [7].

DFT has been used for understanding and studying the stability of new compounds in previous documents [8, 9]. Generally, a new compound is considerably longer than that in a stable orbital at a constant energy level. The electron exchange and correlation of geometry optimization, electronic structure, and optical properties were determined by using a general approximation gradient (GGA) with the interpolation formula [10]. An ultra-soft potential provided by the Vanderbilt optimization method defines the interaction between the electron and ion. In a plane wave basis, the electronic valence wave characteristics are extended to a 16 eV power reduction. In addition to DFT, Fourier power values can also be used for the indigenous signature of any compound [11, 12]. For different compounds and the same for the same compounds, the four spectral picks are unique. Studying the pureness, stability and other intrinsic characteristics of the compound, which can be directly seen at the peaks of Fourier, can benefit us. Therefore, there is an attempt to synthesize Cu_2O nanoparticles using *Datura metel L.* in the current research. UV-Vis, XRD, and FT-IR used to characterize the synthesized nanoparticles and further the compound stabilization has calculated by DFT method. In addition, the calculated energies, thermodynamic characteristics (such as enthalpies, entropies, Gibbs-free energies), modeled structures of complexes, crystals, and clusters, and predicted yields, rates, and regio- and stereospecificity of reactions are also studied.

Experimental

Materials & Methods

The homogeneous *Datura metel L.* leaves collected from farmland on Krishnankoil, Tamil Nadu, India and Copper nitrate ($Cu(NO_3)_2$) purchased from SRL chemicals Mumbai, India, used without any further purification for the synthesis of Cu_2O nanoparticles. *Datura metel L.* leaves dried at room temperature up to brown after then grained by mortar and pestle. The prepared powder consumed for all the characterization and double distilled (DD) water was used throughout the experiment.

Dust and organic moieties contain in leaves of *Datura metel L.* cleaned through the process of washing in tap water followed by DD water after than leaves cut into small pieces. 10 mg of leaves poured into the 100 ml of DD water boiled at 60℃ for 20 min in a magnetic stirrer with the speed of 70 rpm. After cooling, the prepared extract solution has filtered through the Whatman No.1 filter paper. This extract was used as a reducing agent in copper oxide nanoparticles (Cu_2O NPs) synthesis.

In this experiment, 20 ml of extract added drop by drop with 100 ml of 3 mM copper nitrate aqueous solution. The reaction mixture of copper nitrate and leaf extract stirrer for 20 min in this mean time the colour of the solution changed from blue to sea green, which indicates the formation Cu_2O NPs. The formed NPs are maintaining the room temperature up to 15 days after that start to obtained black precipitation. The prepared NPs are filtered and dried at 60˚C for 3 hrs.

Characterization

The UV-Vis absorption spectra are recorded on Shimadzu UV–1800 suited with 10 mm quartz cuvette. XRD measurements carried out on Brucker Eco D8 Advance diffractometer with Cu-Kα radiation (λ= 1.54060 Å). FTIR analysis was performed at room temperature on IRTracer-100 Shimadzu.

Results And Discussion

Spectral Characterization

The inhomogeneous electron gas (the Born–Oppenheimer approximation) is a collection of interacting point electrons traveling quantum–mechanically in the potential region of a set of atomic nuclei that are considered to be static. The independent electron approximation, Hartree theory, and Hartree-Fock theory are the most common approximation schemes used to solve such models. However, over the last thirty years or so, another approach-Density Functional Theory (DFT)-has become increasingly popular for the solution of such problems. This approach has the advantage of being able to solve a wide variety of problems with high precision while still being computationally simple. Density functional theory can be used to measure the electronic structure of atoms, molecules, and solids (DFT). Its aim is to use quantum mechanics' fundamental laws to obtain a quantitative understanding of material properties.

Using traditional electronic structure approaches, the Schrödinger equation of N interacting electrons moving in an external, electrostatic potential is solved (typically the Coulomb potential generated by the atomic nuclei). However, there are major disadvantages to this approach: (1) the problem is nontrivial even for small numbers N, and the resulting wave functions are complicated objects; and (2) the computational effort increases exponentially with increasing N, rendering the description of larger systems prohibitive. DFT takes a different approach, using the one-body density as the fundamental variable instead of the many-body wave function. Density-functional theory is computationally feasible also for large systems since the density n(r) is a function of only three spatial coordinates (rather than the 3N coordinates of the wave function). A significant development influenced spectral analysis methodology, as the numerical approach was improved by Cooley and Tukey in 1965, known as the Fast Fourier Transformation. The continuum of power density or power range indicates the value of the Fourier process in spectral analysis. The function of autocorrelation of a continuous signal plays an important role as well. The Fourier transform of a finite continuous and their relation to infinite, continuous signals will provide the Dirichlet condition and zero means for the continuous operation. The experimental measures of the compound in our paper are limited to a limited amount of time. By multiplying the infinite continuous recording by a data window as defined, the record duration can be limited to a certain period T.

$$W(\alpha) = \sqrt{\frac{2}{\pi}}\frac{T}{2}\frac{sin(\frac{T}{2}\alpha)}{\frac{T}{2}\alpha} \quad (1)$$

The window in fourier integral leads to the identity as

$w(t) = 1$ for $|t| \leq T/2$ (2)

The Fourier transform of this product is the transformation of the infinite record which is paired with transformations of the window when multiplying the infinite record. The Convolution Theorem establishes this relationship, which affirms that:

$F[f(t).w(t)] = F(\alpha) * W(\alpha)$ (3)

Discrete-time Fourier transform (DTFT) is helpful in calculating the diffracted wave information and the obtained peaks tell us all about the molecular design's properties without having to measure the molecular structure. The DTFT is in the direction of x, y, z for a given compound.

$$C = \frac{1}{abc}\int_0^a\int_0^b\int_0^c \rho(x,y,z)\, e^{-j\left(\frac{2\pi h}{a}x+\frac{2\pi h}{a}y+\frac{2\pi h}{a}z\right)} dxdydz \quad (4)$$

The p(x,y,x) gives the density distribution of the crystalline state of the compound and (a,b,c) represent the edge length in the (x,y,z) directions. The DTFT biosynthesis analysis of Cu_2O as shown (Fig. 1) reveals a distinct difference in the spectral density peak for the three experiments. DTFT peaks shown above indicate that the peak value of 1100 is unique to the synthesized compound and that of the previous compound, the lower peak of 200 is. The sharp rise in maximum value also indicates that the compound is more active and reactive than the other compound.

UV-Vis Analysis

The optical properties of biomolecules loaded Cu_2O NPs were analyzed through UV-Vis absorbance spectra. Fig. 2 shows the optical absorbance spectra of the Cu_2O NPs. The formation of Cu_2O NPs confirmed by the colour change of copper nitrate aqueous solution from bluish green to sea green when adding of *Datura metel L.* leaf extract shown (Fig. 3). The SPR absorbance peak was found at 790 nm by the oscillation of electrons on the surface of the Cu_2O NPs, which is clearly revealing the reduction of Cu_2O NPs. The formed Cu_2O NPs absorbance peak at 790 nm shows the electronic d-d transitions making by the Cu^{2+} ions in d orbital, in this kind of absorption favored for the extended lifetime of photogenerated carriers [13]. The serious of alkaloids present on the *Datura metel L.* extract such as hyoscyamine, atropine is exhibited the characteristic absorption band at 200-350 nm in UV-Vis spectra corresponds to π-π* transition [14]. The bandgap energy of prepared Cu_2O nanoparticles is 2.98 eV from Tauc's plot analysis. This bandgap energy well suited for solar cell and optical device applications according to the report of earlier researcher. Awed et al., 2019 has achieved 2.98 eV for nonlinear optical susceptibility through annealing process and Singh et al., 2004 has attained the same bandgap energy for nanocrystalline CdTe film for electroluminescent display devices [15, 16].

XRD Analysis

Crystallinity, size, and phase of the biosynthesized Cu_2O NPs were determined through XRD analysis and their diffraction pattern shown (Fig. 4). Biosynthesized Cu_2O NPs have characteristic diffraction peaks at 2θ angle 22.77°, 25.08°, 26.54°, 29.48°, 31.28°, 32.95°, 36.47°, 38.67°, 42.19°, 47.66°, 51.62°. Here, the observed diffraction reflections peaks at 29.48°, 36.47°, 42.19°, 51.62° indicates the presence of Cu_2O NPs and indexed by Bragg's reflections (110), (111), (200), and (211). According to the JCPDS Card No: 77-0199 the mentioned lattice planes such as (110), (111), (200) are exhibit primitive lattice structures of Cu_2O NPs. Similar kinds of Cu_2O NPS XRD diffractogram are reported by some other researchers for various plant extract [2, 6, 17]. The remaining unassigned peaks and background noises in the XRD pattern represented by the star symbol, which reveals the *Datura metel L.* biomolecules, encapsulated around the Cu_2O NPs [18]. The prepared Cu_2O NPs average crystallite size is 19.56 nm calculated from the result of XRD analysis using Debye – Scherer's equation.

$$D = \frac{k\lambda}{\beta \cos\theta} \quad (5)$$

In this case, k is the dimensionless shape factor taken as 0.9, λ known as X-ray wavelength, β is line broadening at half the maximum intensity (FWHM) and θ is the Bragg angle. This result illustrated biomolecules are well bound with Cu_2O nanoparticles during synthesis and *Datura metel L.* extract is one of the promising candidates for reduction and stabilization of Cu_2O NPs.

Fourier Transform Infrared Spectroscopy Analysis

Phytochemicals present on the plant extract and the formation of Cu_2O were identified through the FTIR spectra analysis. The IR spectra of Cu_2O NPs compared with *Datura metel L.* is shown (Fig. 5). The FTIR spectrum (Fig. 5b) *Datura metel L.* leaf extract shows a broad absorption band at 3406 cm^{-1} which is due to the O-H stretching mode of phenol and alcohols. The peak at 2937 cm^{-1} indicates C-H stretching of alkyl groups and strong peaks 1651 cm^{-1} show the C=C stretching vibration of carboxylic groups. The peaks at 1546 cm^{-1} reveal that the C-N stretch of aliphatic amines and peaks at 1406, 1359, and 1317 cm^{-1} are representing C-C stretch (in-ring) of aromatics, N=O bending vibration of nitro compounds, C-N stretch of aromatic amines, respectively. The peaks that appeared at 1105, and 1068 cm^{-1} are belong to the C-N stretch of aliphatic amines. The peaks at 752, 621, and 526 cm^{-1} are show the existence of C-Cl stretch alkyl halides, C-H bends alkanes, and C-I stretches aliphatic iodo compounds. The FTIR spectrum of Cu_2O NPs showed again the presence of O-H stretching mode of phenol and alcohols and C-H stretching of alkyl groups at 3404, and 1620 cm^{-1}, which supports the idea of phenol, alcohols, and alkyl group, are free from Cu_2O NPs formation. The peaks at 1409, 1359, and 1317 cm^{-1} on Cu_2O NPs represent a diminishment of C-C stretch (in-ring) of aromatics, N=O bending vibration of nitro compounds, C-N stretch of aromatic amines, respectively. After bioreduction, peak shifts have occurred at 752 to 709 cm^{-1} on C-Cl alkyl halides, 621 to 650 cm^{-1} on C-H bend of alkanes, and 526 to 609 cm^{-1} on C-I stretch in aliphatic iodo compounds. Above mentioned biocompounds are acting as a capping agent as well as

bound along with the Cu_2O nanoparticles. The disappearance of peaks at 2937, 1546, 879 cm^{-1} and newly formed peaks at 1043, 999 cm^{-1} confirms the C-H stretching of alkyl, C-N stretch of aliphatic amines, N-H bending vibration of nitro compounds, and C-OH of carboxylic acid are responsible for structural changes on NPs formation. The strong peaks obtained at 819 cm^{-1} and the existence of new peaks at 499 cm^{-1} are correspond to the characteristic formation of Cu_2O NPs (Fig. 5a) [19]. Particularly aliphatic amines in *Datura metel L.* leaf extract are mainly responsible for the reduction of copper ions into Cu_2O NPs.

Density Functional Theory Analysis

The optical properties of a molecule or crystal are among the most useful classes of properties that can predict distinctive characteristics. These can be used to locate wavelengths of optical radiation based on its electronic structure either in the absorption or emission spectrum. DFT lets us calculate these properties, related to electron motion evolution under electric field control. DFT is the theory of differential and functional functions. The spectrum data are shown (Fig. 6). NUM is first standardized with [01] which Gaussian has reoriented to speed up the two calculations of electron energy models. The internal nuclear energy has been measured using the spectral data measurement. The next step is to measure every single electron transaction using the Hamiltonian Fock matrix. Once we know the propagation of the electron, we measure the angular momentum of the electrons that are then used to detect an electron's energy gap.

The energy of the synthesized compound stabilized over some time to a constant value of 16.6378 eV and remained the same indicating compound stability. As shown in Fig. 6. The initial fluctuation is caused by the excitation of the electron that tends to return the electron to its normal condition in time. The oscillation reaction shows that the compound is erratic, but as the proposed compound can be shown, its behavior is very stable.

Computational modeling

Calculation of the thermodynamic and surface characteristics of Cu_2O thin films at all temperatures was carried out using MERA software with periodic boundary conditions along with a, b and c axes of Cu_2O unit cell like it were described in [20, 21] and applied in studying organic, inorganic and combined systems in [20-37].

The MOPS algorithm has been used to model oxyhydrate gel formation [20, 25, 29], crystal structures of triosmium clusters [21, 23, 24, 28, 30, 33, 35], organic molecule complexation during chemical reactions [31], protein affinity [34], and crystal structures and interaction energies of gas hydrates [26, 37]. Calculated energies, thermodynamic properties (such as enthalpies, entropies, and Gibbs-free energies), modeled structures of complexes, crystals, and clusters, and predicted yields, rates, and regio- and stereospecificity of reactions were all in good agreement with experimental results.

The structures hyoscyamine and atropine were optimized at the DFT B3LYP 6-311G (d,p) level of theory. Then, the UV-Vis spectrum was calculated using TD DFT B3LYP 6-311G (d,p) which shows the absorption band is 253.3 nm that in good agreement with the experimental data.

The structure of cuprite [38] (Crystallography Open Database ID 1000063) was taken as the initial structure for the computer simulation of Cu_2O nanoparticles (cubic syngony, space group Pn m, a = b =c = 4.252(2), α = β = γ = 90°).

1000 multiplications of the crystal cell in random directions were performed to the composition $Cu_{2474}O_{1237}$ (this composition corresponds to the experimental size of the particles) and the structure with the minimum energy is chosen. Calculation using the Bragg's equation showed that the resulting modelled nanoparticles should have diffraction reflections peaks at 2θ angle 29.69°, 36.57°, 42.49°, 52.69°, 61.65°, 69.90°, 73.86°, 77.74°, 85.35°. The first four reflections are in good agreement with the experimental diffractogram and correspond to reflections (110), (111), (200), and (211) that show a good quality of the simulation.

The initial structure of atropine and hyoscyamine in an aqueous solution (they are similar, since atropine is a racemate and hyoscyamine is an L-isomer of the same compound) modeled within the MOPS software [20, 25, 29] with the continual account of the solvent influence shown (Fig. 7a). The structure contains the intramolecular hydrogen bond =O…H-O with a length of 2.22 Å.

Subsequently, the modeling of the complex of this nanoparticle with hyoscyamine and with atropine was carried out. The calculated Gibbs free energy of the complex formation is -179.4 kJ/mol. The structure and conformation of atropine (hyoscyamine) remain almost unchanged during the formation of the complex. The complex is formed by three short contacts (Fig. 7b). Two of them are carried out by carbonyl oxygen with two copper atoms of nanoparticles (2.16 and 2.19 Å). These bifurcate interactions become possible due to a defect in the surface of the nanoparticles, when two copper atoms at once turn out to be with a lack of valence. The third contact is the hydrogen bond of the hydroxyl hydrogen of atropine with the oxygen of the nanoparticle surface (2.09 Å). The intramolecular hydrogen bond =O…H-O is retained, but slightly extended to 2.37 Å.

Conclusions

A simple and cost-effective method has been proposed to the synthesis of Cu_2O nanoparticles at room temperature within the reaction time of 30 minutes and abundant, the unappreciated plant of Indian surroundings (*Datura metel L.*) extract utilized as a reducing and stabilizing agent. The UV-Vis analysis shows Cu_2O NPs formation at 790 nm through the making of cu^{2+} ions transition in d-orbital. The result of the XRD pattern reveals that biomolecules of *Datura metel L.* encapsulation on synthesized Cu_2O NPs and found in crystalline nature with an average crystallite size of 19.56 nm. This biomolecules encapsulation is validated by FTIR characterization, the aliphatic amines in *Datura metel L.* responsible for the reduction of Cu_2O NPs, and their Phytochemicals are effectively utilized as a bio-capping agent

and it has been bound along around the Cu_2O NPs. The synthesized compound was tested using DFT and Fourier power spectrum for energy band stability as well as for spectral signatures. These two algorithmic evaluations have enabled us to calculate the stability and unique spectral signature of the proposed Cu_2O compounds. In the first time, we successfully applied spectral characterization with Fourier transform for the biosynthesized Cu_2O NPs and highlighted their spectrum. High transformation of the high frequency of spectral characterization suggests that synthesized Cu_2O NPs to be in more active and reactive than other compound but oscillation reactions are erratic as well as their stability is very stable in behavior even after 10 iterations of density functional theory analysis. Moreover, the present report is used to study the stabilization of nanoparticles in various solar cell, wastewater treatment, and biomedical applications.

Declarations

Author's Declarations

The authors declare no conflict of interest.

Acknowledgments

The project was supported by Ministry of Science and Higher Education of Russia (Grant no. FENU-2020-0019). Authors acknowledged Kalasalingam Academy of Research and Education, Krishnankoil, Tamilnadu, India.

Authors' Contributions

Experimental and characterization of green synthesized Cu_2O nanoparticles using *Datura Metel L* done by KC and supervised by KG, KK, MGR and RT. Theoretical studies performed by KG, VM, VP and MG and supervised by VP and VM. Manuscript written by KC and checked by all authors.

Data Availability All data generated during this study are included in this published article

Funding

The project was supported by Ministry of Science and Higher Education of Russia (Grant no. FENU-2020-0019).

Ethical Approval Not applicable.

Consent to Participate Not applicable.

Consent for Publication Not applicable.

Conflict of interest The authors declare that they have no known competing financial interests.

References

1. Azhar W, Khan AR, Muhammad N, Liu B, Song G, Hussain A, Yasin MU, Khan S, Munir R, Gan Y (2020) Ethylene mediates CuO np-induced ultrastructural changes and oxidative stress in arabidopsis thaliana leaves. Environ. Sci. Nano 7:938-953. https://doi.org/10.1039/C9EN01302D
2. Jadhav MS, Kulkarni S, Raikar P, Barretto DA, Vootlac SK, Raikar US (2018) Green biosynthesis of CuO & Ag–CuO nanoparticles from malus domestica leaf extract and evaluation of antibacterial, antioxidant and DNA cleavage activities. New J. Chem 42: 204-213. https://doi.org/10.1039/C7NJ02977B
3. Kargar A, Jing Y, Kim SJ, Riley CT, Pan X, Wang D (2013) ZnO/CuO Heterojunction branched nanowires for photoelectrochemical hydrogen generation. ACS Nano 7(12):11112-11120. https://doi.org/10.1021/nn404838n
4. Wongrakpanich A, Mudunkotuwa IA, Geary SM, Morris AS, Mapuskar KA, Spitz DR, Grassian VH, Salem AK (2016) Size-dependent cytotoxicity of copper oxide nanoparticles in lung epithelial cells. Environ. Sci. Nano 3:365-374. https://doi.org/10.1039/C5EN00271K
5. Awed AS, El-Ghamaz NA, El-Nahass MM, Zeyada HM (2019) Linear and nonlinear optical properties of alizarin red S thin films. Indian J Phys 93:861-868. https://doi.org/10.1007/s12648-018-01359-6
6. Siddiqui VU, Ansari A, Chauhan R, Siddiqi WA (2021) Green synthesis of copper oxide (CuO) nanoparticles by punica granatum peel extract. Materials Today Proceedings 36: 751-755. https://doi.org/10.1016/j.matpr.2020.05.504
7. Nasir B, Baig MW, Majid M, Ali SM, Khan MJI, Kazmi STB, Haq I (2020) Preclinical anticancer studies on the ethyl acetate leaf extracts of Datura Stramonium and Datura Inoxia. BMC Complement Med Ther 20:188. https://doi.org/10.1186/s12906-020-02975-8
8. Haunschild R, Barth A, French BA (2019) Comprehensive analysis of the history of DFT based on the bibliometric method RPYS. J Cheminform 11:72. https://doi.org/10.1186/s13321-019-0395-y
9. Fermi E (1928) Eine Statistische Methode Zur Bestimmung Einiger Eigenschaften Des Atoms und ihre Anwendung auf die Theorie des periodischen Systems der Elemente. Z. Physik 48:73-79. https://doi.org/10.1007/BF01351576
10. Haunschild R, Barth A, Marx W (2016) Evolution of DFT studies in view of a scientometric perspective. J Cheminform 8:52. https://doi.org/10.1186/s13321-016-0166-y
11. Ciaccio EJ, Biviano AB, Whang W, Coromilas J, Garan H (2011) A new transform for the analysis of complex fractionated atrial electrograms. BioMed Eng OnLine 10:35. https://doi.org/10.1186/1475-925X-10-35
12. Mesgaran SD, Eggert A, Höckels P, Derno M, Kuhla B (2020) The use of milk Fourier transform mid-infrared spectra and milk yield to estimate heat production as a measure of efficiency of dairy cows. J Animal Sci Biotechnol 11:43. https://doi.org/10.1186/s40104-020-00455-0
13. Luo Z, Jiang H, Li D, Hu L, Geng W, Wei P, Ouyang P (2014) Improved photocatalytic activity and mechanism of $Cu_2O/N–TiO_2$ prepared by a two-step method. RSC Adv 4:17797-17804.

https://doi.org/10.1039/C3RA47973K

14. Ramalechume C, Shamili P, Krishnaveni R, Swamidoss CMA (2020) Synthesis of copper oxide nanoparticles using tree gum extract, its spectral characterization, and a study of its anti- bactericidal properties. Materials Today Proceedings 33:4151-4155. https://doi.org/10.1016/j.matpr.2020.06.587
15. Grad L, Novotny Z, Hengsberger M, Osterwalder J (2020) Influence of surface defect density on the ultrafast hot carrier relaxation and transport in Cu_2O photoelectrodes. Sci Rep 10:10686. https://doi.org/10.1038/s41598-020-67589-z
16. Singh RS, Rangari VK, Sanagapalli S, Jayaraman V, Mahendra S, Singh VP (2004) Nano-structured CdTe, CdS and TiO_2 for thin film solar cell applications. Sol. Energy Mater. Sol. Cells 82:315-330. https://doi.org/10.1016/j.solmat.2004.02.006
17. Sasidharan D, Namitha TR, Johnson SP, Jose V, Mathew P (2020) Synthesis of silver and copper oxide nanoparticles using myristica fragrans fruit extract: antimicrobial and catalytic applications. Sustain. Chem. Pharm 16:100255. https://doi.org/10.1016/j.scp.2020.100255
18. Sarkar J, Chakraborty N, Chatterjee A, Bhattacharjee A, Dasgupta D, Acharya K (2020) Green synthesized copper oxide nanoparticles ameliorate defence and antioxidant enzymes in lens culinaris. Nanomaterials 10:312. https://doi.org/10.3390/nano10020312
19. Anand GT, Sundaram SJ, Kanimozhi K, Nithiyavathi R, Kaviyarasu K (2021) Microwave assisted green synthesis of CuO nanoparticles for environmental applications. Materials Today Proceedings 36:427-434. https://doi.org/10.1016/j.matpr.2020.04.881
20. Sukharev YI, Potemkin VA, Markov BA (2001) Autowave processes of forming gels as a cause of the coloring of oxyhydrate gels (the chromatic effect) of some rare earth metals (yttrium, gadolinium). Colloids Surf. A 194:75-84. https://doi.org/10.1016/S0927-7757(01)00757-9
21. Potemkin VA, Maksakov VA, Kirin VP (2003) Conformational states of triosmium clusters with aminoacid ligands: a theoretical study. J. Struct. Chem 44:741-747. https://doi.org/10.1023/B:JORY.0000029809.88411.8b
22. Potemkin VA, Krasnov VP, Levit GL, Bartashevich EV, Andreeva IN, Kuzminsky MB, Anikin NA, Charushin VN, Chupakhin ON (2004) Kinetic resolution of (±)-2,3-dihydro-3-methyl-4H-1,4-benzoxazine in the reaction with (S)-naproxen chloride: a theoretical study. Mendeleev Commun 14:69-70. https://doi.org/10.1070/MC2004v014n02ABEH001887
23. Potemkin VA, Maksakov VA, Kirin VP (2004) Theoretical study of the conformations of triosmium clusters with a chiral carane ligand. J. Struct. Chem 45:405-409. https://doi.org/10.1007/s10947-005-0006-9
24. Potemkin VA, Maksakov VA, Korenev VS (2005) Theoretical study of the conformational states of triosmium clusters with a chiral pinane ligand. J Struct. Chem 46:43-48. https://doi.org/10.1007/s10947-006-0007-3
25. Sukharev YI, Avdin VV, Lymar AA, Belkanova MY, Potemkin VA (2006) Directions in structure formation of oxyhydrate gels of zirconium and rare earth elements. J. Struct. Chem. 47:151-155. https://doi.org/10.1007/s10947-006-0280-1

26. Aladko EY, Ancharov AI, Goryainov SV, Kurnosov AV, Larionov EG, Likhacheva AY, Manakov AY, Potemkin VA, Sheromov MA, Teplykh AE, Voronin VI, Zhurko FV (2006) New type of phase transformation in gas hydrate forming system at high pressures. Some experimental and computational investigations of clathrate hydrates formed in the SF6–H_2O system. J. Phys. Chem. B 110:21371-21376. https://doi.org/10.1021/jp061698r
27. Grishina MA, Potemkin VA, Bartashevich EV, Sinyaev AN, Rusinov GL, Latosh NI, Ganebnykh IN, Koryakova OV, Ishmetova RI (2006) Modeling of 1,2,4,5-tetrazine complexes with organic amines. J. Struct. Chem 47:1155-1160. https://doi.org/10.1007/s10947-006-0438-x
28. Potemkin VA, Maksakov VA, Korenev VS (2007) Theoretical study of the conformational states of triosmium clusters with a chiral μ-1-NH pinane ligand. J. Struct. Chem 48:225-230. https://doi.org/10.1007/s10947-007-0036-6
29. Avdin VV, Lymar AA, Batist AV, Nikitin EA, Belkanova MY, Potemkin VA (2007) Structure formation in heavy metal oxyhydrates at low rates of gel formation, J. Struct. Chem 48:747-752. https://doi.org/10.1007/s10947-007-0114-9
30. Korenev VS, Kirin VP, Maksakov VA, Virovets AV, Tkachev SV, Potemkin VA, Agafontsev AM, Tkachev AV (2007) Triosmium cluster with the bridging aminooxime derivative of pinane: synthesis, crystal structure and conformational analysis. Russ. J. Coord. Chem 33:594-600. https://doi.org/10.1134/S1070328407080088
31. Shchur IV, Khudina OG, Burgart YV, Saloutin VI, Grishina MA, Potemkin VA (2007) Synthesis, structure, and complexing ability of fluoroalkyl-containing 2,2'-(biphenyl-4,4'-diyldihydrazono)-bis(1,3-dicarbonyl) compounds. Russ. J. Org. Chem 43:1781-1787. https://doi.org/10.1134/S107042800712007X
32. Grishina MA, Potemkin VA, Matern AI (2008) Theoretical study of acridane oxidation reactions. J. Struct. Chem 49:7-12. https://doi.org/10.1007/s10947-008-0002-y
33. Maksakov VA, Pervukhina NV, Podberezskaya NV, Afonin MY, Potemkin VA, Kirin VP (2008) X-ray and conformation analysis of the new trinuclear cluster of osmium Os3(μ,η2-OCC6H5)(CO)9. J. Struct. Chem 49:894-900. https://doi.org/10.1007/s10947-008-0154-9
34. Kuzmicheva GA, Jayanna PK, Eroshkin AM, Grishina MA, Pereyaslavskaya ES, Potemkin VA, Petrenko VA (2009) Mutations in Fd phage major coat protein modulate affinity of the displayed peptide. Protein Eng., Des. Sel 22:631-639. https://doi.org/10.1093/protein/gzp043
35. Potemkin VA, Ivshina NN, Maksakov VA (2009) Theoretical Study of the conformational features of triosmium clusters. J. Struct. Chem 50:143-151. https://doi.org/10.1007/s10947-009-0202-0
36. Ivshina NN, Bartashevich EV, Potemkin VA, Grishina MA, Ishmetova RI, Rusinov GL, Latosh NI, Slepukhin PA, Charushin VN (2010) Changes in the vibrational characteristics of substituted 1,2,4,5-tetrazines after complexation with 1,2,3-benzotriazole: A theoretical study. J. Struct. Chem 50:1053-1058. https://doi.org/10.1007/s10947-009-0155-3
37. Manakov AY, Likhacheva AY, Potemkin VA, Ogienko AG, Kurnosov AV, Ancharov AI (2011) Compressibility of gas hydrates. ChemPhysChem 12:2476-

2484. https://doi.org/10.1002/cphc.201100126
38. Neuburger M. C (1931) Präzisionsmessung der Gitterkonstante von Cuprooxyd Cu_2O. Zeitschrift für Physik 67:845-850. https://doi.org/10.1007/BF01390765

Tables

Table 1 FTIR wavenumbers and their corresponding functional group analysis of Cu_2O synthesized by *Datura metel L*

Wavenumbers (cm^{-1})		Vibrational assignments	Functional groups
Datura metel L	Cu_2O NPs		
3406	3404	O-H stretching	phenol, alcohols
1651	1620	C=C stretching	carboxylic groups
1406	1409	C-C stretch (in-ring)	Aromatics
1359	1359	N=O bending	nitro compounds
1317	1317	C-N stretch	aromatic amines
1105	1124	C-N stretch	aliphatic amines
1068	943	C-N stretch	aliphatic amines
752	709	C-Cl stretch	alkyl halides
621	650	C-H bend	Alkanes
526	609	C-I stretch	aliphatic iodo
2937	-	C-H stretching	Alkyl
1546	-	C-N stretch	aliphatic amines
879	-	N-H bending vibration	nitro compounds
-	819	Characteristic formation of Cu_2O NPs	
-	499		

Figures

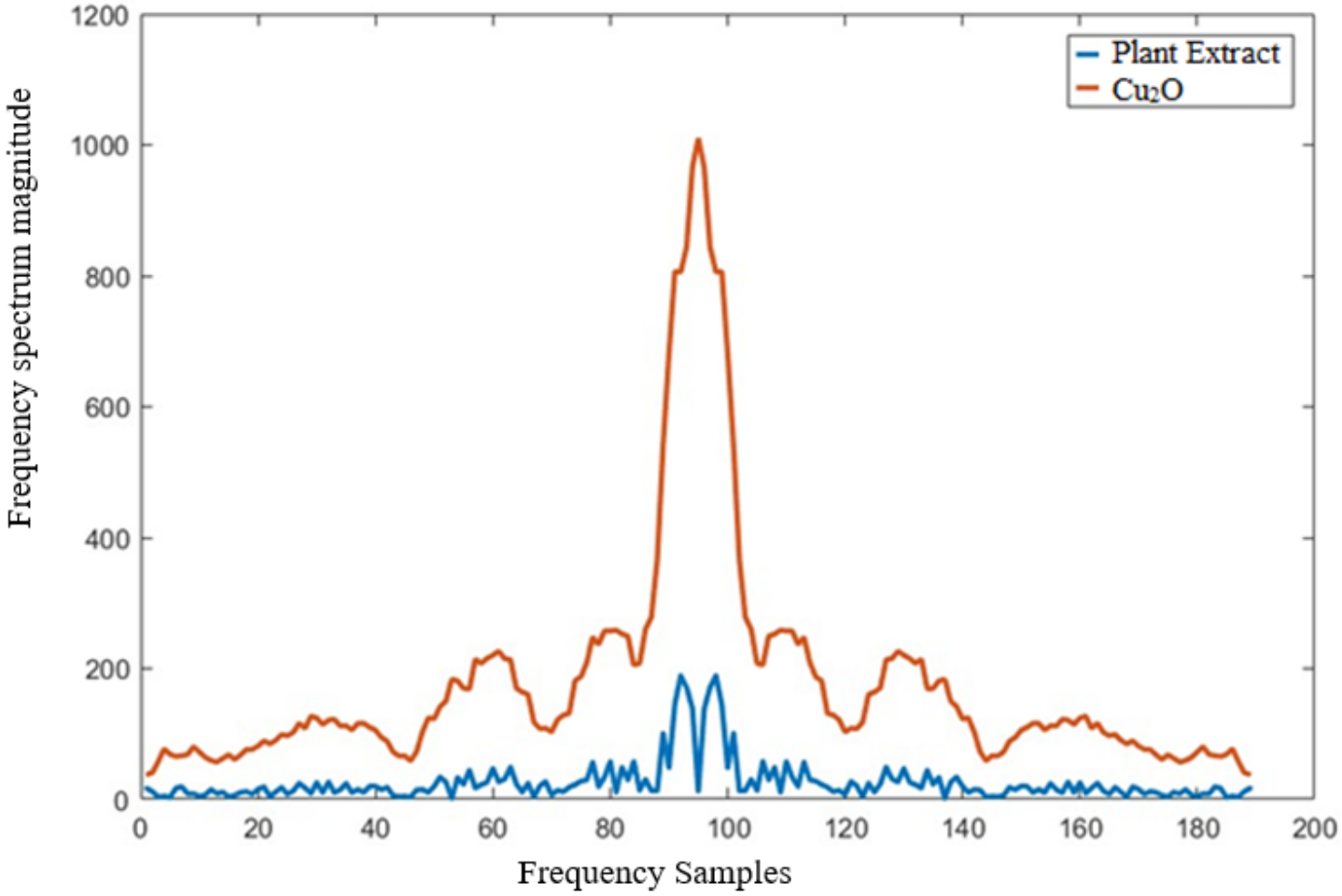

Figure 1

Displays the spectral characterization with a Fourier Transform of the proposed Cu2O compound results. The higher transformation of the high frequency suggests the biosynthesis of Cu2O

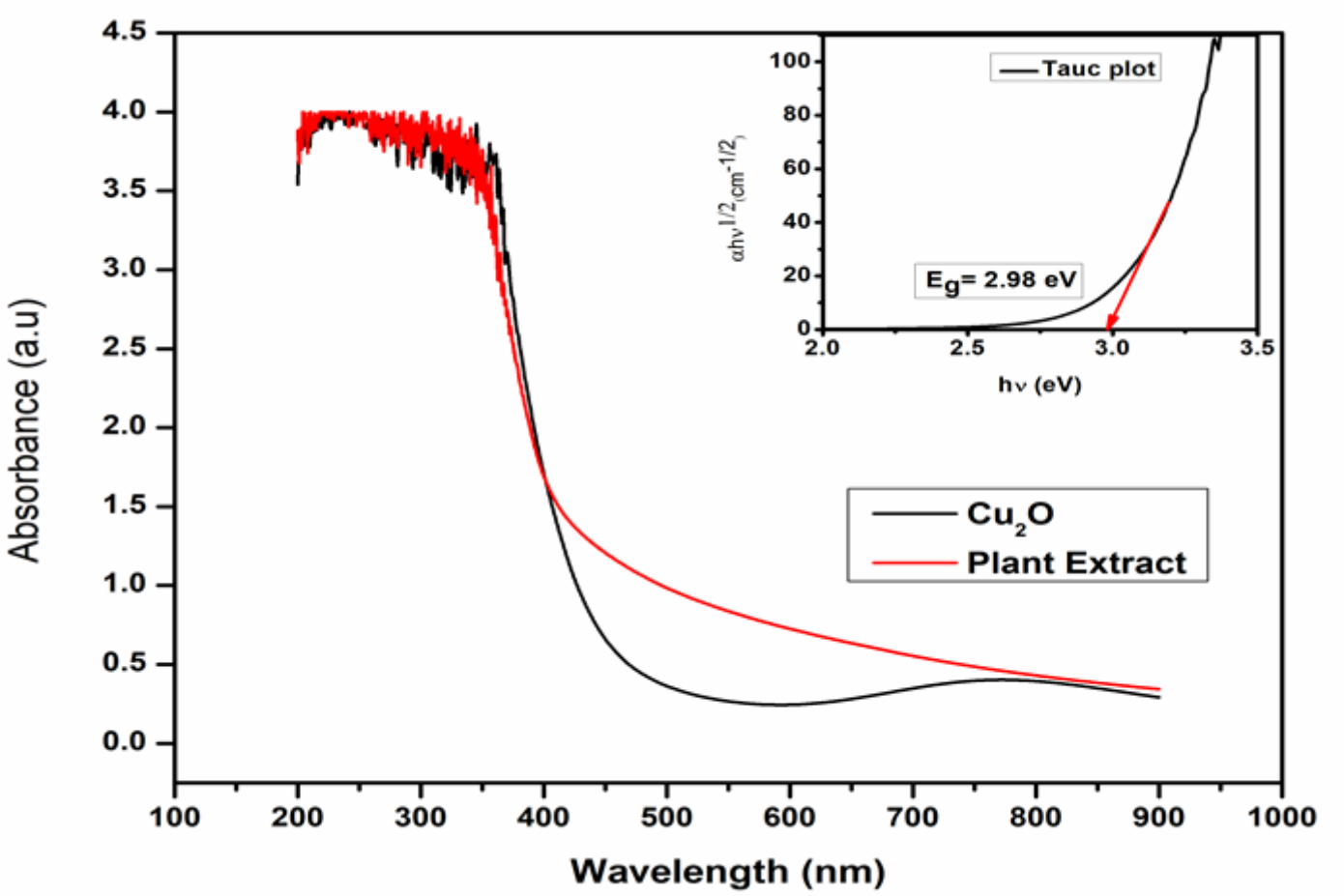

Figure 2

UV-Vis absorption spectra of Cu2O NPs

Figure 3

Formation of Cu2O NPs

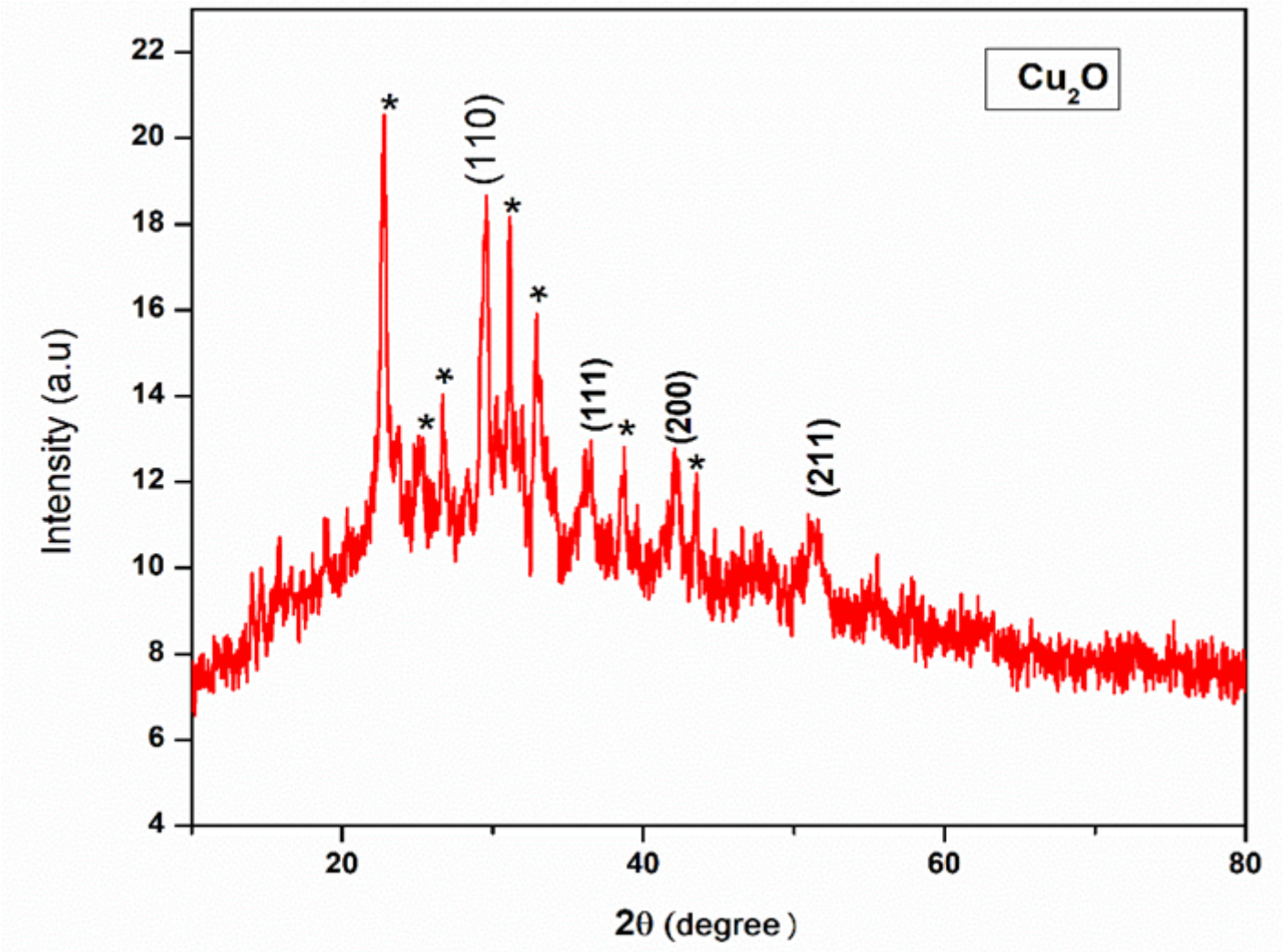

Figure 4

XRD analysis of Cu2O NPs

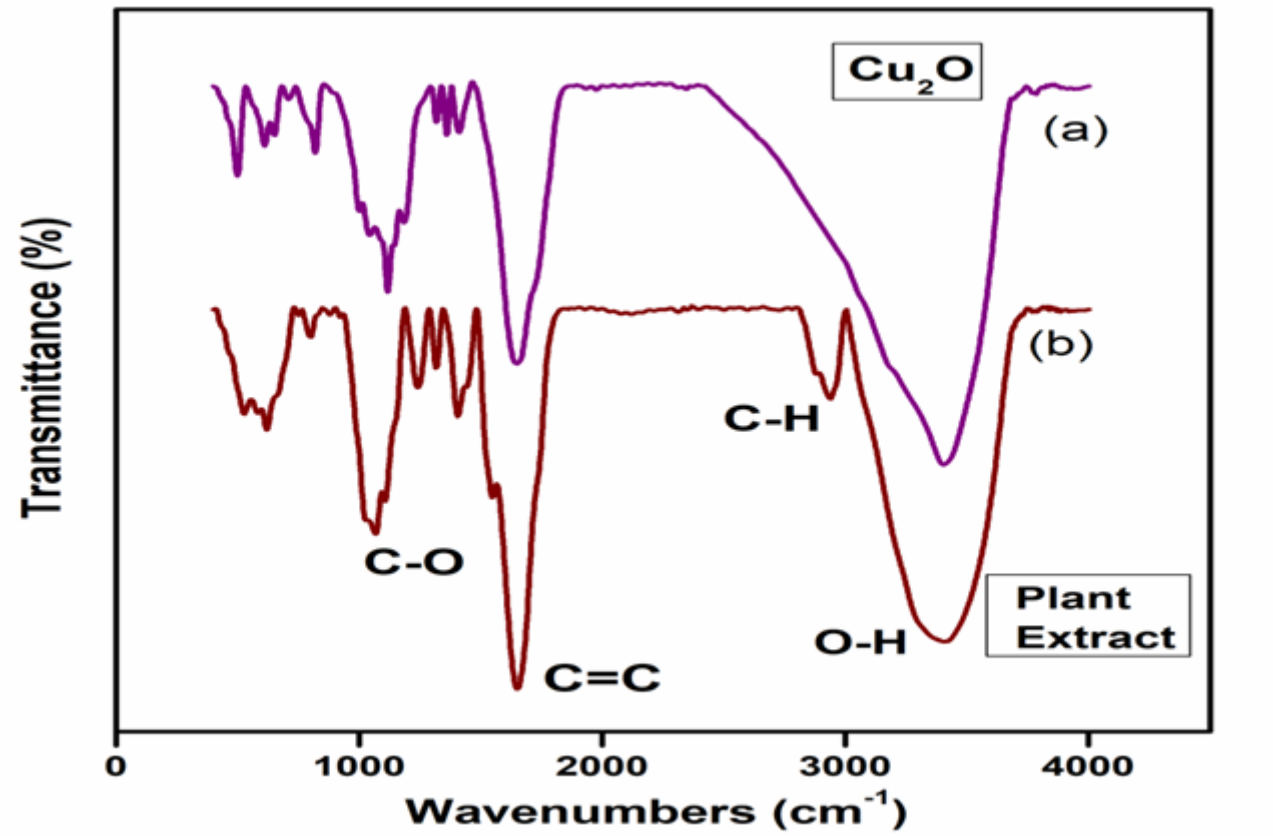

Figure 5

FTIR spectra (a) Cu2O NPs and (b) Plant extract

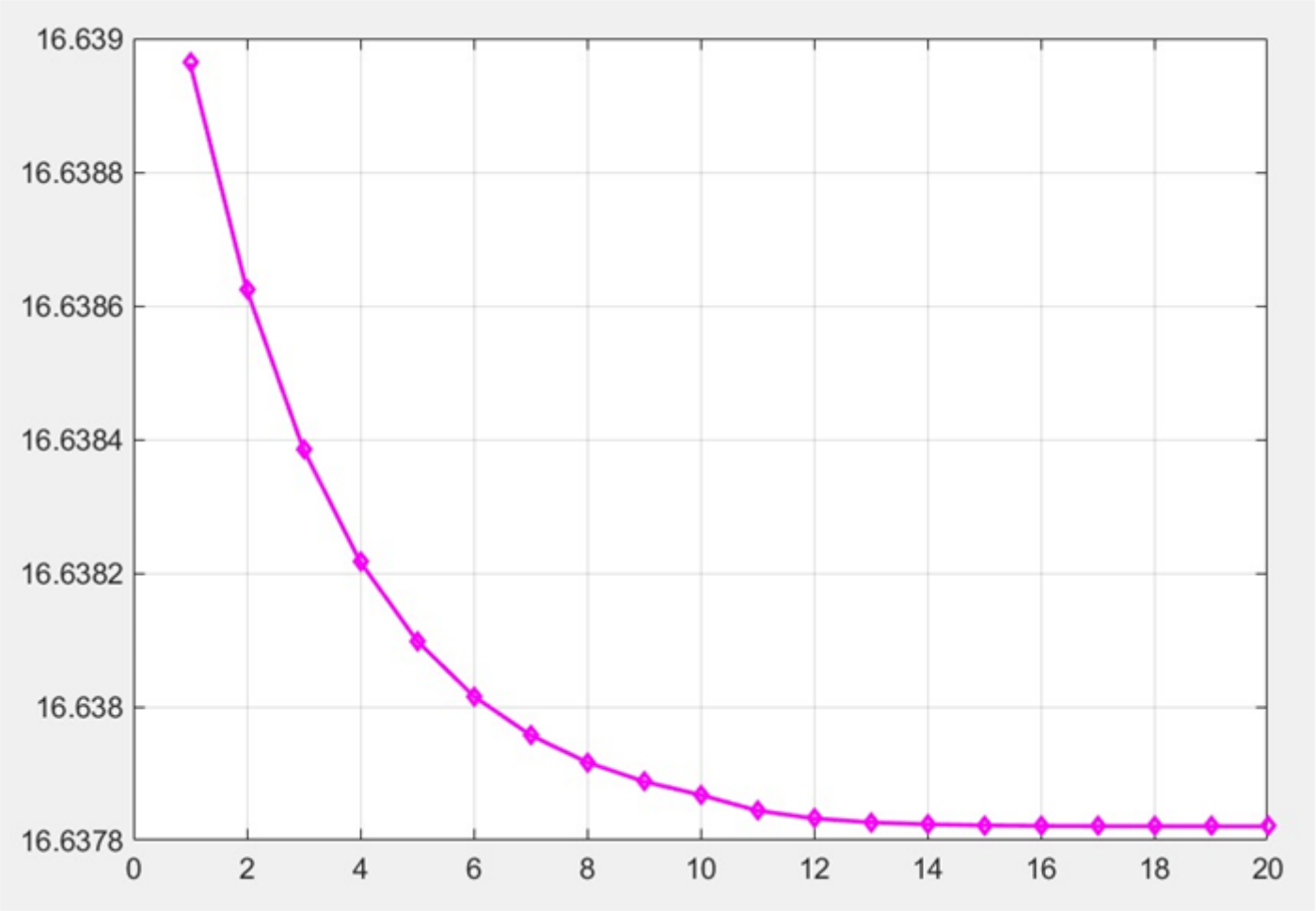

Figure 6

Energy (eV) versus DFT iterations show the compound's stability after 10 iterations, since the energy levels obtain a constant value and remain the same

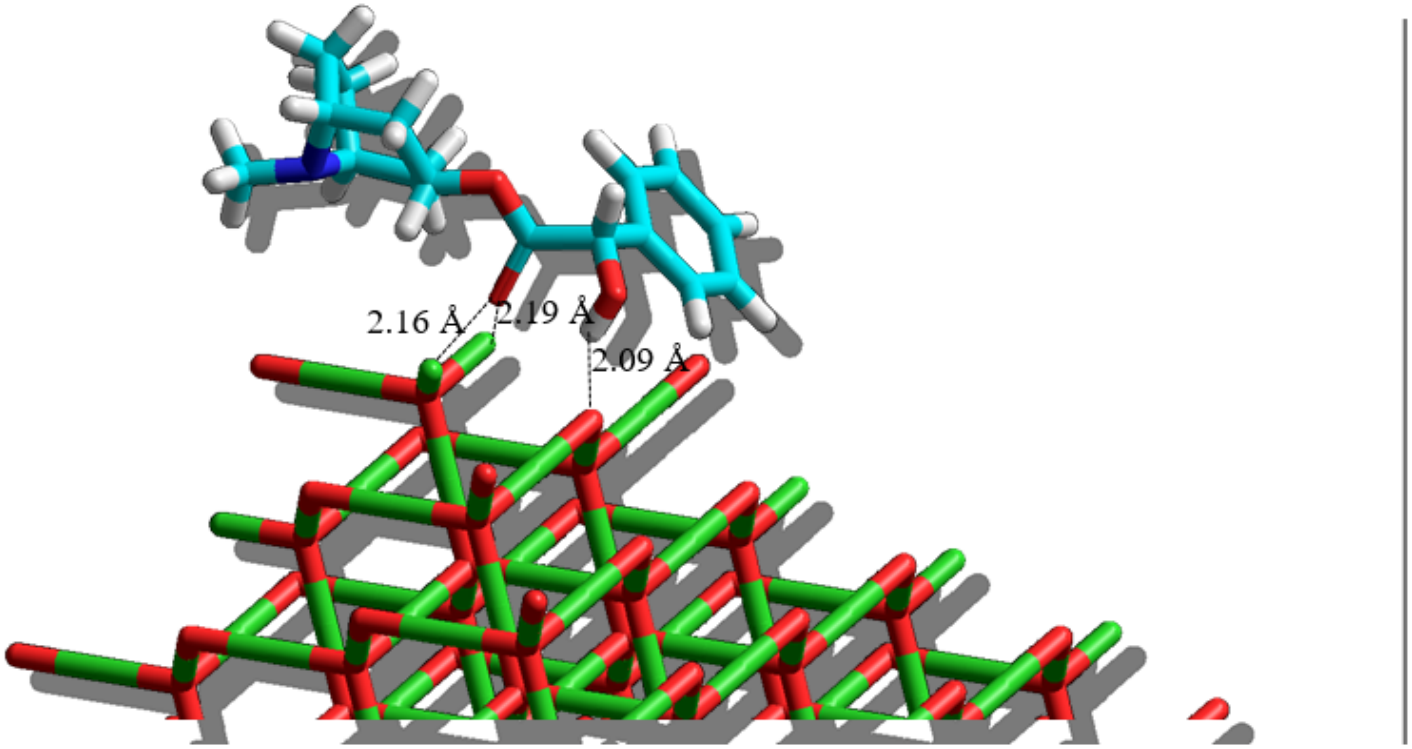

Figure 7

The structure of a) atropine and b) its complex with the fragment of Cu2O nanoparticles